REACTIVE CONTROL AND ITS OPERATION LIMITS IN RESPONDING TO A NOVEL SLIP IN GAIT

Feng Yang and Yi-Chung Pai

Department of Physical Therapy
University of Illinois at Chicago
Chicago, IL 60612

Corresponding author: Yi-Chung (Clive) Pai, PhD
Department of Physical Therapy
University of Illinois at Chicago
1919 West Taylor St., Room 426 (M/C 898)
Chicago, Illinois 60612, USA
Tel: +1-312-996-1507
Fax: +1-312-996-4583
E-mail: cpai@uic.edu

ABSTRACT

The purposes of this study were: (1) to examine the reactive control of the resultant joint moments at the lower limbs in response to a novel and unannounced slip; (2) to establish individualized forward-dynamics models; and (3) to explore personal potential by determining the *operation limits* of these moments at each lower limb joint, beyond which the resulting motion at this or other joints will exceed its/their normal range(s). Ten young subjects' kinematics and kinetics, collected during regular walking and during their first exposure to a novel and unannounced slip, were randomly selected from an existing database. An inverse-dynamics approach was applied to derive their (*original*) resultant joint moments, which were then used as input to establish forward-dynamics models, each including an individualized 16-element foot model to simulate ground reaction force. A simulated annealing (SA) algorithm was applied to modify the original moments, so that the subsequent output (*baseline*) moments can closely reproduce these subjects' *recorded* motion. A systematic alteration of the baseline moments was employed to determine the operation limits. The results revealed that the subjects reactively increased the hip extensor and knee flexor moments and reduced their ankle plantar flexor moments of their single-stance limb following slip onset. The "baseline" correction of the original moments can reach as much as 21% of the original moments. The analysis of the operation limits revealed that these individuals may be able to further increase their knee flexors more so than increase the hip extensors or reduce ankle plantar flexors before causing abnormal joint movement. Such systematic approach opens the possibility to properly assess an individual's rehabilitation potential, and to identify whether this person's strength is the limiting factor for stability training.

Keywords: Muscle strength; Postural response; Feedback; Feed-forward; Optimization; Stability; Recovery; Falls.

INTRODUCTION

Falls are a major cause of injury and even death in adults aged 65 and over[31]. Falls initiated by a slip account for about one quarter of all falls among elders[21,23]. To resist slip-related falls during walking, the central nervous system (CNS) must reactively modify the resultant moments of the lower limbs that can provide stability recovery while support upright posture against gravity[12,18,28,37]. A better understanding of one's reactive control of the joint moments at the lower limbs during recovery from a slip is imperative in order to properly assess this individual's risk of future falls and to effectively prevent them from occurring. Such individualized *reaction-based* approach has more resemblance and hence more relevance to the real life situations than *volitional-performance-based* evaluation common in clinical practice[7,32].

Resultant joint moments result directly from muscle activation that is governed by a descending motor program initiated from and modulated by various motor centers of the CNS. Comparisons between slip response and regular walking of the resultant joint moments, which are traditionally derived through an inverse-dynamics approach, can often reveal the mechanism of the recovery from the slip[12,18]. It has been postulated that increased knee flexor and hip extensor moments in the stance limb might be two primary reactive responses required to stabilize the human body and to avoid a slip-related fall in gait[12].

The inverse-dynamics approach does not directly quantify the causal relationship between the joint moments and the motion state (i.e., the position and velocity) of body segments. Further, the inverse-dynamics approach is unable to assess, control, or eliminate the confounding impact of the kinematic variability, which is common in empirical sampling, on the inversely-derived joint moments. Even small inter-subject differences in the initial posture (or body segment motion state) could yield large subsequent differences in joint moments. Moreover, the joint

moments derived from the traditional inverse-dynamics approach often cannot reproduce the original body segment movement, when such derived joint moments and forward dynamics are used to drive the same individualized human model. The existence of such discrepancy, which likely results from inherent measurement errors[22], not only raises doubts on the validity of this approach, but also presents challenge for the simulation attempt.

Because of these limitations, computer simulation based on forward dynamics has been used to investigate human movement mechanisms, primarily due to its ability to quantitatively analyze the changes in muscle forces or resultant joint moments that exclusively lead to the changes in movements[1,17]. This type of analysis is often conducted by systematically altering the muscle force or the joint moments in the forward-dynamics simulation, then calculating the resulting changes in the motion state of the body segments in walking[3,24] and running[14]. A core requirement of forward-dynamics simulation is the input of the time histories of the joint moments necessary to drive the forward-dynamics simulation. Yet, for these joint moments to reproduce the originally recorded joint motion, one of the various forms of optimization has to be applied to resolve aforementioned dilemma[13,17,25,26,30]. Still, none of them has been employed to develop individualized models and to investigate the reactive control of slip recovery in gait. Equally unclear is the personal potential for further improving his/her stability control that would be critical to the prevention of falls.

The purposes of this study were therefore: 1) to examine the reactive control of the resultant joint moments at the lower limbs in response to a novel and unannounced slip; 2) to establish individualized forward-dynamics models; and 3) to explore personal potential by determining the *operation limits* of these moments at each lower limb joint, beyond which the resulting motion at this or other joints would exceed normal range. An inverse-dynamics approach would derive

individual subjects' (*original*) resultant joint moments of the lower limbs, which would then be used as input to establish forward-dynamics models including an individualized 16-element foot model to simulate ground reaction force (GRF). In this process, a simulated annealing (SA) algorithm would be applied to modify the original moments, so that the subsequent output (*baseline*) moments can closely reproduce these subjects' originally recorded motion. Finally, the operation limits of these individualized models would be examined.

MATERIALS AND METHODS

The data of 10 young adults [mean ± standard deviation (SD) age: 24.4 ± 2.9 yr, range 22-32 yr; 5 females] were randomly selected from an existing database collected during normal walking, and during their first exposure to a novel and unannounced slip in walking[8,9]. The mean ± SD body height and mass were 1.69 ± 0.07 m and 64.7 ± 15.5 kg, respectively. All subjects have given written informed consent to the experimental protocol approved by the Institutional Review Board.

Subjects were told that a slip would be possible but no information was given as to where, when, or how the slip would occur. Each subject wore a full body harness system to protect against the impact of an actual fall. Following approximately 10 regular walking trials at each subject's self-selected speed, a right-foot slip trial was induced by electronically releasing a low-friction moveable platform embedded in a 7-m long walkway with surrounding decoy platform(s)[38]. The first slip trial and its preceding regular walking trial were analyzed and compared to identify the reactive response to the slip.

Kinematics and GRF were gathered using an eight-camera motion capture system (Motion Analysis Corporation, Santa Rosa, CA) and four synchronized force-plates (AMTI, Newton,

MA), respectively. Specifically, 26 markers were affixed at vertex, ears, rear neck (the spinous process of the 7th cervical vertebra), shoulders (the acromion of the scapulae), midpoint of the right scapula, elbows (the lateral humeral epicondyles), wrists (the radial styloid processes), sacrum, greater trochanters, mid-thighs, knees (the lateral femoral epicondyles), mid-legs (the tibial tubercles), ankles (the lateral malleoli), heels (calcaneal tuberosities), and the 5th metatarsal heads. Based on these markers' position, the centers of bilateral ankle, knee, and hip joints, and the center of mass of the pelvis and trunk can be constructed[33]. The sagittal-plane joint angles can then be computed by using inverse kinematics, with the standard anatomical position as 0° for all joints[17].

An individualized, 7-segment, sagittal-plane model, consisting of both feet, shanks, thighs, and HAT (head, arm, and trunk)[36], was developed in this study (Fig. 1). For each subject's individual model, the segment lengths and the location of its center of mass (COM) were calculated from the relative distance between pairs of joint centers[16]. The slipping (right) foot was the base segment for the whole model. Each anatomical joint in the model was actuated by resultant joint moments, and has its own peak flexor/extensor moments[2] and range-of-motion limits[11] (Table 1).

The single-stance phase immediately after slip onset is an important period for slip recovery, and is the focus of the present study[37]. Resultant joint (*original*) moments of the lower limb during single-stance phase were first calculated by using a traditional inverse-dynamics approach based on the same individualized model (Fig. 2). The *original* joint moments were then applied as inputs to be modified by forward dynamics with the aid of an optimization routine to better match the experimentally-measured body kinematics and kinetics (Fig. 2). The inverse- and forward-dynamics computations were both based on the same set of equations of motion:

$$\mathbf{M}(\mathbf{q})\ddot{\mathbf{q}} + \mathbf{H}(\mathbf{q},\dot{\mathbf{q}}) + \mathbf{G}(\mathbf{q}) + \mathbf{F}(\mathbf{q},\dot{\mathbf{q}}) = \boldsymbol{\tau} \quad (1)$$

where, $\mathbf{q} = (x, y, \theta_i)$, $i = 1, 2, 3, \cdots, 7$ represents the generalized coordinates of the human model (Fig. 1). Coordinates x, y, and θ_1 specify the position and orientation of the right foot with reference to the inertial reference frame. Joint angles θ_i (i = 2, 3, 4, …, 7) correspondingly indicate the angels of the ankle, knee, hip of the stance limb and the hip, knee, and ankle of the swing limb. **M** is the mass matrix, **H** represents the matrix of Centrifugal and Coriolis terms, **G** is the matrix of the gravity term, **F** the GRF term, and $\boldsymbol{\tau}$ the joint moments. The generalized position, velocity, and acceleration ($\mathbf{q}/\dot{\mathbf{q}}/\ddot{\mathbf{q}}$) were derived from experimentally-measured kinematic data and input to the inverse-dynamics computation, but were the output of the forward-dynamics simulation. For the GRF, its values, obtained from the force plate measurement, were the input to the inverse-dynamics computation, while it was calculated from a foot contact model (see below) in the forward-dynamics simulation. The equations of motion were derived based on Newton-Euler method[33] and solved by a custom-developed program in Matlab (The Mathworks Inc., Cambridge, MA) for the inverse dynamics. They were derived using SD/Fast (PTC, Needham, MA) based on Kane's method and integrated using a Runge-Kutta-Feldberg variable-step integrator for the forward simulation[6]. The initial conditions, including the initial position, velocity, and the slipping velocity of right foot were calculated from the experimental data at the beginning of single-stance phase (i.e., the left foot liftoff).

A foot contact model was constructed for forward-dynamics simulation to represent the interactions of the right foot with the ground when there is no actual experimental data available in model prediction. The ground is represented by a flat rigid line (Fig. 1). A total of 16 independent visco-elastic elements with identical properties uniformly arranged down the midline of the sole were used to model the impact and friction effects of the foot with the

ground[19]. These properties, i.e., the spring and damping coefficients were optimized to best reproduce the GRF and individualized for each subject. Each element permits deformation perpendicular to the floor. The vertical GRF and the center of pressure were calculated as the summary of the vertical force in each element resulted from its vertical deformation. The horizontal GRF was calculated as the product of the resultant vertical GRF and the coefficient of friction (COF) between the sole and the ground, which was set as < 0.05 based on experimental results[38]. The GRF would be zero for the swing limb, for which there was no motion-induced foot deformation, or it would vary as function of the foot kinematics for the stance limb.

The resultant joint moments for the forward-dynamics simulation were computed using the following relationship[36]:

$$\tau_i = \begin{cases} u_i \ t \ \Gamma_i^E & u_i \ t \ \geq 0 \\ u_i \ t \ \Gamma_i^F & u_i \ t \ < 0 \end{cases} \quad (2)$$

where τ_i, u_i, , and Γ_i are the joint moments, activation level, and the physiological maximum moments of the i^{th} joint , respectively. The superscripts E and F represent extensor and flexor for knee and hip, or plantar flexor and dorsiflexor for the ankle.

The objective of the optimization routine was to modify the resultant joint moments of the lower limbs so that the output kinematics and GRF from the forward-dynamics model could closely replicate each subject's measured body kinematics and kinetics (Fig. 2). The SA algorithm[15] was used to seek the best activation levels, $u(t)$ and spring/damping coefficients, which served as the *control* variables to minimize the following *objective function*:

$$\min f = \sum_{i=1}^{m} w_i \cdot \int_{t_i}^{t_f} \left[Y_i \ t \ - \hat{Y}_i \ t \ \right]^2 dt \quad (3)$$

where $Y_i(t)$ represents the measured kinematic or kinetic variable *i* at time instant *t* from the experiments, $\hat{Y}_i(t)$ is the simulation data corresponding to $Y_i(t)$, and w_i is weight for the i^{th} term. The specific quantities evaluated in Eq. (3) were the displacements of the stance heel, the stance foot, the stance and swing ankle, knee, and hip angles, and GRF's under the stance foot, leading in a total of *m* = 11 variables in Eq. (3). The final output of this dynamic optimization procedure included the activation-time history necessary for constructing the *baseline* moments at each joint as well as individualized spring/damping coefficients (see Appendix A).

In order to determine operation limits of the baseline moments, these control variables ($\boldsymbol{\tau}_{\text{baseline}}$) were altered systematically above or below the level of the baseline moments throughout the single-stance phase, one joint at a time, by adding or subtracting a fixed interval of $\Delta\tau = 10^{-3}$ Nm/kg.

$$\begin{aligned}&\mathbf{M}(\mathbf{q}+\Delta\mathbf{q})(\ddot{\mathbf{q}}+\Delta\ddot{\mathbf{q}})+\mathbf{H}(\mathbf{q}+\Delta\mathbf{q},\dot{\mathbf{q}}+\Delta\dot{\mathbf{q}})\\&+\mathbf{G}(\mathbf{q}+\Delta\mathbf{q})+\mathbf{F}(\mathbf{q}+\Delta\mathbf{q},\dot{\mathbf{q}}+\Delta\dot{\mathbf{q}})=\boldsymbol{\tau}_{\text{baseline}}+\Delta\boldsymbol{\tau}\end{aligned} \tag{4}$$

As shown in Eq. (4), the forward-dynamics simulation will be conducted with the altered joint moments ($\boldsymbol{\tau}_{\text{baseline}} + \boldsymbol{\Delta\tau}$) as the input and the altered generalized coordinates ($\mathbf{q} + \boldsymbol{\Delta q}$) as the output. This process of augmentation continued until the point at which the left foot contacted the ground or at which any joint angle from simulation became anatomically unrealistic. When the joint angles begin to exceed 1 SD above the standard range of motion for that particular joint[11], or its moments exceed the limit of the corresponding maximum muscle strength[2] (Table 1), the simulation would be terminated at that alteration level.

The closeness of the fit of the optimal simulated kinematics/kinetics and experimental data was estimated by their correlation coefficient ρ. The root mean square (RMS) of the residual error

between the simulated results and experimental data was adopted to indicate the magnitude of the error. The closeness of the original moments and baseline moments was also evaluated by their ρ and RMS. The operation limits of all joints, in both lower limbs, were examined using a 2 (side) × 3 (joint) analysis of variance with Bonferroni-corrected post hoc *t*-tests in SPSS 17.0 (SPSS Inc., an IBM Company, Chicago, IL). A significance level of 0.05 was used for all analyses.

RESULTS

The reactive control of the CNS for slip recovery was characterized by an increase in the stance hip extensor and knee flexor moments, and a reduction in the plantar flexor moments from those of regular walking (Fig. 3). The inhibitory effect on the stance ankle plantar flexors was especially rapid and pronounced, reaching a magnitude close to 1.2 Nm/kg in just half of the single-stance phase.

The experimental error was successfully reduced by the optimization routine in each individualized forward-dynamics model, such that the baseline moments could closely reproduce the originally recorded joint motion (Fig. 4). The mean (± 1 SD) of RMS between the original and uncorrected joint angles were 5.3° (± 1.3°), 4.4° (± 0.9°), and 1.6° (± 0.3°) at stance hip, knee, and ankle, respectively. The corresponding ρ are -0.86 (± 0.15), -0.95 (± 0.09), and -0.89 (± 0.12). After the application of the optimization routine, the RMS of *all* joint angles, the right heel displacement, and the GRF reduced to 2.1° (± 0.9°), 6.6 (± 2.4) mm, and 32.5 (± 17.1) N [or 5.6 (± 3.0)% body weight], respectively. The corresponding ρ values respectively were 0.98 (± 0.03), 0.97 (± 0.03), and 0.94 (± 0.04). The mean (± SD) of RMS between the original and the baseline moments were 0.10 (± 0.11) Nm/kg, 0.07 (± 0.09) Nm/kg, and 0.02 (± 0.05) Nm/kg for stance hip, knee, and ankle, respectively. The corresponding ρ were 0.77 ± 0.16, 0.94 ± 0.10,

and 0.92 ± 0.09, respectively. The "baseline" correction of the original moments can reach as much as 21% of the original moments.

Finally, although the operation limits varied substantially across the bilateral joints (Table 2, Fig. 6), they accounted for only a fraction of the limits of muscle strength (Fig. 5). Except for ankle plantar flexors, the joints of the swing limb can tolerate at least twice as much alteration as its stance limb counterpart ($p < 0.001$, Table 1). For example, the operation limits at the swing knee [-471, 93]$\Delta\tau$ and hip [-281, 194]$\Delta\tau$ were respectively 3.47 and 4.31 fold larger than that of the stance limb (Table 2). The type of failure caused by excessive moments at each joint was consistent across all subjects (Table 2, Fig. 6). An excessive extensor (or plantar flexor) moments at any joint of the stance limb and at the swing hip caused hyper extension at the stance knee (Fig. 6-a), whereas excessive flexor moments at these same joints led to hyper dorsiflexion of the stance limb (Fig. 6-b). Excessive extensor (or plantar flexor) moments at the swing knee and ankle resulted in ipsilateral ankle hyper plantar flexion (Fig. 6-c). In contrast, excessive flexor (or dorsiflexor) moments at these two joints caused hyper dorsiflexion in the ipsilateral ankle (Fig. 6-d).

DISCUSSION

Upon encountering a novel and unannounced slip, the CNS indeed has to reactively and drastically modify its ongoing motor program for regular working across every joint of the stance limb. These changes in motor control were very robust, far exceeded the differences between the corrected (baseline) and uncorrected (original) resultant moments at each joint, that is, the differences possibly resulted from measurement error (Fig. 3). However, these differences, as well as those between the corrected and uncorrected joint motion, clearly existed at every joint in each subject, and underscored the importance of the optimization routine that was employed to

minimize the error and to improve the validity of the simulation (Fig. 3). Such development provided the foundation for the model simulation and resulting analysis on the operation limits that shed new light on quantitative assessment of an individual person's performance.

These subjects' reaction to slip in the stance (slipping) limb could be characterized by a shift into hip extensor and knee flexor dominance (Fig. 3). During the push-off phase in regular walking, the plantar flexors of the ankle joint usually increase their activation to produce as much as 1.2 Nm/kg[34]. Following a slip, such activation was mostly inhibited to yield moments less than 0.1 Nm/kg (Fig. 3). The posture response generated by the knee and hip, including increased knee flexor and hip extensor moments, could appropriately come from the biarticular portion of the posterior muscle group of hamstrings, allowing the subject to rotate the shank forward and to pull the foot back towards the hip while reducing its slip velocity[39].

These findings were in general agreement with previous studies on gait-slip (Fig. 7), which could be induced on a contaminated floor surface[12] or by a motorized force plate[18]. Nonetheless, the details on the stance knee-flexor dominance differ somewhat from these previous studies[12,18] (Fig. 7). Specifically, the stance knee had a biphasic extensor-flexor moments in one[18] or extensor-dominant moments in the other[12]. The stance ankle plantar flexor dominance found in our study is the same as that reported by one study[18], but differs from that of another study[12], in which the stance ankle appears to be dorsiflexor-dominant.

These differences between the present results and previous ones may result from the different mechanisms used to induce the slip. In the study conducted by Ferber and associates[18], the forward perturbation was induced by a motorized force platform. This preset mechanism controls the velocity and the distance of the perturbation and further constrains the spontaneous

movement of the slipping foot. On the other hand, the contaminated floor surface was less slippery in the previous study with a COF reportedly around 0.12[12], which was much greater than 0.05, the upper limit in the present study. As a result, the distance and the peak velocity of the forward slip, which characterize the intensity of the slip, differed among these three studies: they were 0.78 m and 2.51 m/s in our study[37], 0.1 m and 0.78 m/s in one[29], and 0.1 m and 0.40 m/s in the other[18], respectively. Given that a small variability in body segment kinematics can be associated with substantial differences in the resultant joint moments, these differences in slip intensities could have accounted for the differences in the joint moment profiles of these studies.

The traditional inverse-dynamics approach has been applied to discover the reactive changes occurring at various lower limb joints[12,18]. Unfortunately, it could not decipher the function nor assess the impact of each of these changes on the control of stability. *It would not be prudent to assume that spontaneous reaction is always functionally correct, meaningful, and significant.* It is unclear, for instance, whether and by how much an increase in the activation of the stance knee flexors leads to an improvement of the COM stability. In contrast, the forward model simulation can determine that such reactive control at the lower limb joints, ~160 ms after the onset of the forward slip, does indeed improve the overall dynamic stability[39]. In fact, computations derived from the forward-dynamics model have shown that for every 1 Nm/kg increase in the knee-flexor moments of the slipping limb, the slip velocity could be reduced by 14.24 m/s, and therefore, the COM stability, a dimensionless variable characterized by the motion state (i.e., the position and velocity) of the COM relative to its base of support[27], could be improved by a factor of 2.99[39].

The forward simulation also revealed, in the present study, that the operation limits only account for a fraction of one's muscle strength limits (without taking into consideration the prospect of

co-contraction). This would lead to a logical conclusion that the muscle strength has not been the limiting factor that causes balance loss in all these cases. This evidence appears to lend support to empirical observation in which the strength test results of those who recovered did not differ from those who fell[20,35]. An individualized human model and the analysis of the operation limits of the resultant moments may be important to address specific clinical problems in rehabilitation because of its ability to assess the reaction of an individual in the presence of a perturbation. Detectable inter-subject variability in the operation limits may be indicative of their potential for improvement. Such variability was similarly noted when the role of individual muscles during the single-stance phase of a spring was investigated by forward-dynamics approaches[5,14].

The operation limits might also provide a basis for the assessment of joint function during recovery from forward slip induced in gait. For example, the potential range for the stance hip to further increase its extensor moments or the ankle to reduce its plantar flexor moments is very limited in comparison to the capacity to reduce the knee extensor moments (Table 2, Fig. 6). Because the increment in hip extensor and the reduction in plantar flexor moments could both potentially improve stability[39] and prevent falls[12] during gait-slip, this suggests that these subjects might have performed maximally in augmenting their stance hip-extensors in their reactive response to a novel and unannounced slip in gait. The operation limits did vary among subjects (Table 2, Fig. 6). Yet, there was a consistent trend in these subjects' reaction to slip, and most of them appeared to have increased their hip and reduced their ankle moments near their corresponding operation limits (40/742 or 5.4% from the hip-extensor increase limit and 2/28 or 7.1% from plantar flexor reduction limit, Table 2) before causing hyper extension at the ipsilateral knee. In contrast, the knee flexor moments had the potential to be further increased (107/236 or 45.3% from knee-flexion increase limit, Table 2) without causing any undesirable

effect.

From one perspective, the optimization approach taken in the present study is a fitting of the joint motion data. It also served other capacity, however, beyond merely a data fitting, which in itself improves the validity of the model simulation. For instance, an ordinary data fitting approach cannot satisfy the need of *predicting* future GRF. In contrast, the individualized 16-element foot contact model generated by the optimization approach supplements the common GRF-dependent relationship generally straddling between body segment motion state and joint moments. Further, the optimization-generated, individualized forward dynamics models are capable of predicting the operation limits at each joint. For the first time, by comparing the limits with well-known muscle strength limitation, investigators can determine, at each person's individual joint, whether muscle strength is indeed a limiting factor in stability recovery.

The present study has limitations. The operation limits in which multiple joint moments (i.e., any two, three, or more) are altered simultaneously have not been investigated. Therefore, the coordinated changes among the lower limb joints were not studied in this present work. As a first step, however, the current analysis is essential to identify the potential exclusively attributable of each joint in recovery from a slip perturbation. Additionally, the focus of the present study only centered on the single-stance phase during slip in gait. Still, beginning from ~160 ms after slip onset, this period consists of robust reactive response from feedback control and it can be critically important in deciding subsequent recovery outcome from the slip[37]. Finally, the current study is only about the first unannounced slip in walking. In previous studies, the subjects' reaction to the slip perturbation is rapidly altered within only a few trials of repeated-slip training, in part due to the proactively improved COM stability before slip onset with feed-forward control[10,28]. Such proactive improvements are often achieved by anteriorly

shifting the COM relative to the base of support, and are often sufficient to avoid a backward balance loss. They would therefore render reactive correction of the lower limb joint moments unnecessary or inconsequential. Perceivably, the reactive knee or hip moment profile could become similar to that of regular walking as movement error diminishes. Nonetheless, such proactive strategy could still require prior knowledge and anticipation of a potential slip or an environmental cue to activate. Regardless, this hypothesis, as well the interaction between feed-forward and feedback control, clearly warrants further investigation.

In summary, this study established an approach for a personalized model to closely reproduce an individual's reaction to a novel and unannounced slip perturbation induced in gait. Such a reaction was characterized by increases in the hip extensor and knee flexor moments and reduction in ankle plantar flexor moments for slip recovery. The present forward-dynamics approach lays down a foundation for the investigation of the mechanistic role that each individual joint plays in such recovery[39]. Lastly, the analysis on operation limits may be applied to assess a person's rehabilitation potential aimed at reactive control to improve stability against slip-related falls.

Acknowledgements

This work was funded by NIH 2R01-AG16727 and R01-AG029616. The authors thank Dr. Frank C. Anderson for contributing his software platform and his earlier consultation, and Debbie Espy for editing the text.

REFERENCES

1. Anderson, E. A., J. B. Ellis, A. J. Weiss. Verification, validation and sensitivity studies in computational biomechanics. *Computer Methods in Biomechanics and Biomedical Engineering*. 10: 171-184, 2006.
2. Anderson, F. C. A dynamic optimization solution for a complete cycle of normal gait: An analysis of muscle function and joint contact force. PhD dissertation, University of Texas at Austin, Austin, Texas. 1999.

3. Anderson, F. C., S. R. Goldberg, M. G. Pandy. Contributions of muscle forces and toe-off kinematics to peak knee flexion during the swing phase of normal gait: an induced position analysis. *J. Biomech.* 37: 731-737, 2004.
4. Anderson, F. C., M. G. Pandy. Dynamic optimization of human walking. *J. Biomech. Eng.* 123: 381-390, 2001.
5. Arnold, A. S., M. H. Schwartz, D. G. Thelen, S. L. Delp. Contributions of muscles to terminal-swing knee motions vary with walking speed. *J. Biomech.* 40: 3660-3671, 2007.
6. Atkinson, L. V., P. J. Harley, J. D. Hudson. Numerical methods with Fortran 77: a practical introduction. Workingham, UK: Addison-Wesley, 1989, 405 pp.
7. Berg, K. O., S. L. Wood-Dauphinee, J. I. Williams, B. Maki. Measuring balance in the elderly: validation of an instrument. *Can. J. Public Health.* 83 Suppl 2: S7-11, 1992.
8. Bhatt, T., Y. C. Pai. Can observational training substitute motor training in preventing backward balance loss after an unexpected slip during walking? *J. Neurophysiol.* 99: 843-852, 2008.
9. Bhatt, T., E. Wang, Y.-C. Pai. Retention of adaptive control over varying intervals: prevention of slip-induced backward balance loss during gait. *J. Neurophysiol.* 95: 2913-2922, 2006.
10. Bhatt, T., J. D. Wening, Y.-C. Pai. Adaptive control of gait stability in reducing slip-related backward loss of balance. *Exp. Brain Res.* 170: 61-73, 2006.
11. Boone, D. C., S. P. Azen. Normal range of motion of joints in male subjects. *Journal of Bone and Joint Surgery*. 61: 756-759, 1979.
12. Cham, R., M. S. Redfern. Lower extremity corrective reactions to slip events. *J. Biomech.* 34: 1439-1445, 2001.
13. Chao, E. Y., K. Rim. Application of optimization principles in determining the applied moments in human leg joints during gait. *J. Biomech.* 6: 497-510, 1973.
14. Chumanov, E. S., B. C. Heiderscheit, D. G. Thelen. The effect of speed and influence of individual muscles on hamstring mechanics during the swing phase of sprinting. *J. Biomech.* 40: 3555-3562, 2007.
15. Corona, A., M. Marchesi, C. Martini, S. Ridella. Minimizing multimodal functions of continuous variables with the "Simulated Annealing" algorithm. *ACM Transactions on Mathematical Software*. 13: 262-280, 1987.
16. de Leva, P. Adjustments to Zatsiorsky-Seluyanov's segment inertia parameters. *J. Biomech.* 29: 1223-1230, 1996.
17. Delp, S. L., F. C. Anderson, A. S. Arnold, P. Loan, A. Habib, C. John, D. G. Thelen. OpenSim: Open-source software to create and analyze dynamic simulations of movement. *IEEE Transactions on Biomedical Engineering*. 54: 1940-1950, 2007.
18. Ferber, R., L. R. Osternig, M. H. Woollacott, N. J. Wasielewski, J.-H. Lee. Reactive balance adjustments to unexpected perturbations during human walking. *Gait & Posture*. 16: 238-248, 2002.
19. Gilchrist, L. A., D. A. Winter. A two-part, viscoelastic foot model for use in gait simulations. *J. Biomech.* 29: 795-798, 1996.
20. Grabiner, M. D., T. M. Owings, M. J. Pavol. Lower extremity strength plays only a small role in determining the maximum recoverable lean angle in older adults. *J. Gerontol. A. Biol. Sci. Med .Sci.* 60A: 1447-1450, 2005.
21. Holbrook, T. L. The frequency of occurrence, impact and cost of musculoskeletal conditions in the United States. *American Academy of Orthopedic Surgeons*. 1984.
22. Kuo, A. D. A least-squares estimation approach to improving the precision of inverse dynamics computations. *J. Biomech. Eng.* 125: 864-874, 1998.

23. Layne, L. A., K. M. Pollack. Nonfatal occupational injuries from slips, trips, and falls among older workers treated in hospital emergency departments, United States, 1998. *Am. J. Ind. Med.* 46: 32-41, 2004.
24. Liu, M. Q., F. C. Anderson, M. G. Pandy, S. L. Delp. Muscles that support the body also modulate forward progression during walking. *J. Biomech.* 39: 2063-2630, 2006.
25. Neptune, R. R., S. A. Kautz, F. E. Zajac. Contributions of the individual ankle plantar flexors to support, forward progression and swing initiation during walking. *J. Biomech.* 34: 1387-1398, 2001.
26. Neptune, R. R., I. C. Wright, A. J. Van Den Bogert. A method for numerical simulation of single limb ground contact events: Application to heel-toe running. *Computer Methods in Biomechanics and Biomedical Engineering*. 3: 321-334, 2000.
27. Pai, Y.-C. Movement termination and stability in standing. *Exerc. Sport Sci. Rev.* 31: 19-25, 2003.
28. Pai, Y.-C., T. Bhatt. Repeated slip training: An emerging paradigm for prevention of slip-related falls in older adults. *Phys. Ther.* 87: 1478-1491, 2007.
29. Redfern, M. S., R. Cham, K. Gielo-Perczak, R. Gronqvist, M. Hirvonen, H. Lanshammar, M. Marpet, C. Y. Pai, C. Powers. Biomechanics of slips. *Ergonomics*. 44: 1138-1166, 2001.
30. Seth, A., M. G. Pandy. A neuromusculoskeletal tracking method for estimating individual muscle forces in human movement. *J. Biomech.* 40: 356-366, 2007.
31. Stevens, J. A., P. S. Corso, E. A. Finkelstein, T. R. Miller. The costs of fatal and non-fatal falls among older adults. *Inj. Prev.* 12: 290-295, 2006.
32. Tinetti, M. E. Performance-oriented assessment of mobility problems in elderly patients. *Journal of the American Geriatric Society*. 34: 119-126, 1986.
33. Vaughan, C. L., B. L. Davis, C. J. O'Connor. Dynamics of Human Gait. Cape Town, South Africa: Kiboho Publishers, 1992, pp 141.
34. Winter, D. A. Overall principle of lower limb support during stance phase of gait. *J. Biomech.* 13: 923-927, 1980.
35. Wojcik, L. A., D. G. Thelen, A. B. Schultz, J. A. Ashton-Miller, N. B. Alexander. Age and gender differences in peak lower extremity joint torques and ranges of motion used during single-step balance recovery from a forward fall. *J. Biomech.* 34: 67-73, 2001.
36. Yang, F., F. C. Anderson, Y.-C. Pai. Predicted threshold against backward balance loss in gait. *J. Biomech.* 40: 804-811, 2007.
37. Yang, F., T. Bhatt, Y.-C. Pai. Role of stability and limb support in recovery against a fall following a novel slip induced in different daily activities. *J. Biomech.* 42: 1903-1908, 2009.
38. Yang, F., Y.-C. Pai. Correction of the inertial effect resulting from a plate moving under low-friction conditions. *J. Biomech.* 40: 2723-2730, 2007.
39. Yang, F., Y.-C. Pai. Role of individual lower limb joints in reactive stability control following a novel slip in gait. *J. Biomech.* 43: 397-404, 2010.

TABLE

Table 1 The limit of moment[2] (normalized to the body mass, Nm/kg) and range of motion[11] (°) for each lower limb joint on both extension (plantar flexion for ankle) and flexion (dorsiflexion for ankle) directions.

	Limit of moment		Range of motion	
	Extension /Plantar flexion	Flexion /Dorsiflexion	Extension /Plantar flexion	Flexion /Dorsiflexion
Hip	4.1	3.3	9.8 ± 6.8	122.3 ± 6.1
Knee	3.8	1.9	0.0	142.5 ± 5.4
Ankle	2.3	0.8	12.6 ± 4.4	56.2 ± 6.1

Table 2 Mean (SD) of the baseline moments at lower limb joints at the left (recovery) foot liftoff, the operation limits of addition or subtraction applied to each subject's (n = 10) moment-time history before any joint angles at any instant of the entire single-stance phase begin to exceed 1 SD above the standard range of motion or their moments exceed the limits of the corresponding muscle strength. Also listed is the type of failure occurring above the maximum alteration. The joint moments and alteration in the joint moments are normalized to the body mass, i.e., in Nm/kg.

Joints	Sides	Baseline moments ($\times 10^{-3}$)	Operation limits			
			Addition		Subtraction	
			Range ($\times 10^{-3}$)	Failure type	Range ($\times 10^{-3}$)	Failure type
Hip	Stance	742 (168)	40 (11)[a,c]	RHKE	-97 (16)[a]	RHDF
	Swing	-298 (140)	194 (20)[b]	RHKE	-281 (32)[b]	RHDF
Knee	Stance	-236 (146)	24 (4)[a]	RHKE	-107 (18)[a]	RHDF
	Swing	101 (48)	93 (18)[b]	LHPF	-471 (35)[b]	LHDF
Ankle	Stance	28 (34)	19 (2)[d]	RHKE	-2 (1)[a,e]	RHDF
	Swing	-13 (21)	16 (5)[b]	LHPF	-15 (6)[b]	LHDF

For the joint moments, positive values indicate extensor or plantar flexor.

[a]: $p < 0.001$ vs. swing side; [b]: $p < 0.001$ vs. other two swing joints; [c]: $p < 0.05$ vs. stance knee;

[d]: $p < 0.01$ vs. stance hip; [e]: $p < 0.001$ vs. other two stance joints;

RHKE: right knee hyper extension exceeding 0°; RHDF: right ankle hyper dorsiflexion exceeding 17°;

LHPF: left ankle hyper plantar flexion exceeding 62.3°; LHDF = left ankle hyper dorsiflexion exceeding 17°.

CAPTIONS

Fig. 1 Schematic of the 7-link, 9-degree-of-freedom, sagittal-plane model of the human body. The vector $\mathbf{q} = [\, x, y, \theta_1, \theta_2, \cdots \theta_7 \,]$ represents the generalized coordinates of the model. Coordinates x, y, and θ_1 specify the position and orientation of the right (stance or slipping) foot, which is the base segment of the model following the left (swing or recovery) foot liftoff after slip onset, with reference to the inertial reference frame (*X, Y, Z*). Joint angles θ_i $(i = 2, 3, 4, \cdots, 7)$ correspondingly specify the angles of the ankle, knee, hip of the stance limb (solid line) and the hip, knee, and ankle of the swing limb (dashed line). The positive *X*-axis is in the direction of forward progression, and the positive *Y*-axis is upward. Positive joint rotation is along the positive *Z*-axis (counterclockwise) for the stance limb (solid line), and its sign is reversed (clockwise) for the swing limb (dashed line).

Fig. 2 Schematic of the procedure to derive joint moments which can reproduce the experimentally measured kinematics (the joint angles and base of support displacement) and kinetics (the ground reaction forces) during a slip in gait. These derived joint moments are called baseline moments. The procedure, including two main parts: forward-dynamics simulation and optimization, was used to modify the original moments which were derived by traditional inverse-dynamics approach from experimental measurements to baseline moments. A simulated annealing (SA) algorithm was used to perform the optimization routine. The iteration process is indicated by the narrow arrow.

Fig. 3 The profile (mean ± SD) of lower limb joint moments across 10 subjects, calculated from an inverse-dynamics (*original* moments, solid line) and from our forward-dynamics approach (*baseline* moments, dashed line), during single-stance phase (single-limb support of the right foot) from left foot liftoff (LLO) to its touchdown (LTD) for right (stance) (a) hip,

(b) knee, and (c) ankle. The instant of LLO typically occurs ~160 ms after slip onset (OS). Also shown are the average joint moments during the single-stance phase of the regular walking trial, across the same subject group (dash-dotted line). The arrows indicate the changes from these moments measured in regular gait, that are reflective of the reactive control at each joint, which these subjects actually had executed in response to a novel and unannounced slip in gait. It is obvious that this response includes increasing hip extensor and knee flexor and reducing ankle plantar flexor moments during the slip trials. The joint moments are normalized to body mass.

Fig. 4 A representative simulation sample of single-stance phase, from left (swing) foot liftoff (LLO) to its touchdown (LTD), for a subject (body mass = 72.6 kg, body height = 1.70 m). The instant of LLO typically occurs ~160 ms after slip onset (OS). This shows that the optimization-derived (*corrected*) results (in dashed line) closely tracked the experimental (*original* in solid line) kinematics and kinetics, by our optimization/forward-dynamics simulation procedure. In comparison, the *uncorrected* kinematics (in dash-dotted line) was computed by forward-dynamics approach without using optimization algorithm to reduce error, which is clearly visible. The kinematics (angular or linear displacement) & the joint moments of the (a & b) hip, (c & d) knee, (e & f) ankle, (g & h) foot, and the horizontal & vertical component of the ground reaction force (GRF) (i & j) are all demonstrated at the right limb. The joint moments are normalized to body mass and the GRF is normalized to body weight, *bw*.

Fig. 5 The group mean (n = 10) of the operation limits for the resultant joint moments of stance (a) hip, (b) knee, and (c) ankle during the entire single-stance phase from left (swing) foot liftoff (LLO) to its touchdown (LTD). During an altered simulation, the joint moments are altered by adding or subtracting a fixed interval $\Delta\tau$ at 10^{-3} Nm/kg. Also shown are the

average baseline moments for each stance side joint across all subjects. For each joint, the greater operation limit is demonstrated. The upper and lower bounds of the operation limits are defined as the maximum allowed alteration size imparted to the baseline moments before the joint angles at any instant of the entire single-stance phase begin to exceed 1 SD above the standard range of motion for that particular joint[11], or their moments exceed the limits of the corresponding muscle strength illustrated by the thin horizontal lines and the values normalized by body mass, i.e., in Nm/kg[2,4].

Fig. 6 Four types of failure encountered in altered simulation: (a) hyper extension at right (stance) knee (RHKE), (b) hyper dorsiflexion at right ankle (RHDF), (c) hyper plantar flexion at left ankle (LHPF), and (d) hyper dorsiflexion at left ankle (LHDF). See Table 2 for detailed definition of failure type. The numbers beneath the stick figures indicate the simulation time in percentage, and the asterisk represents the COM position. The triangle is the starting position of the right heel at left foot liftoff. The altered simulation would fail once the perturbed joint angles deviated by 1 SD from the corresponding joint's range of motion. Small circles on the stick figures were used to identify the joint which encountered the unrealistic movement. To illustrate the joint movement clearly, the small circles were enlarged.

Fig. 7 Comparison of the group mean of lower limb joint moments at stance side between our study and those reported by other researchers[12,18]. All three sets of joint moments were derived by an inverse-dynamics approach during the single-stance phase from left (swing) liftoff (LLO) to its touchdown (LTD) in gait-slip. Joint moments are normalized to body mass in Nm/kg.

FIGURES

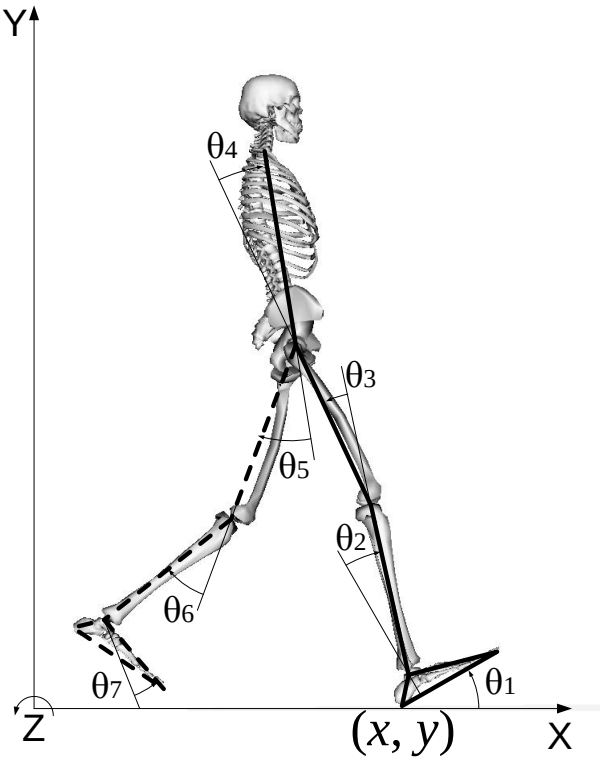

Fig. 1 [Yang and Pai, 2010]

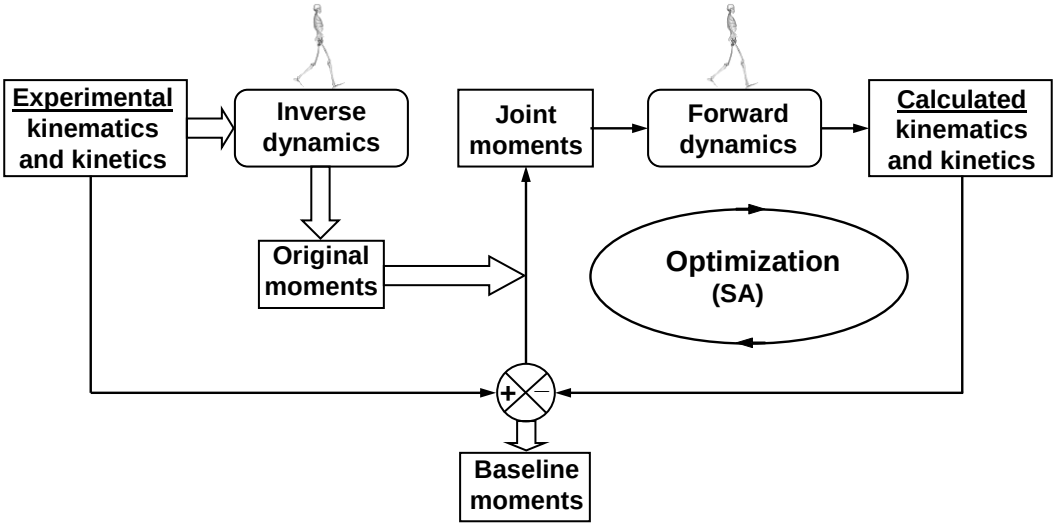

Fig. 2 [Yang and Pai, 2010]

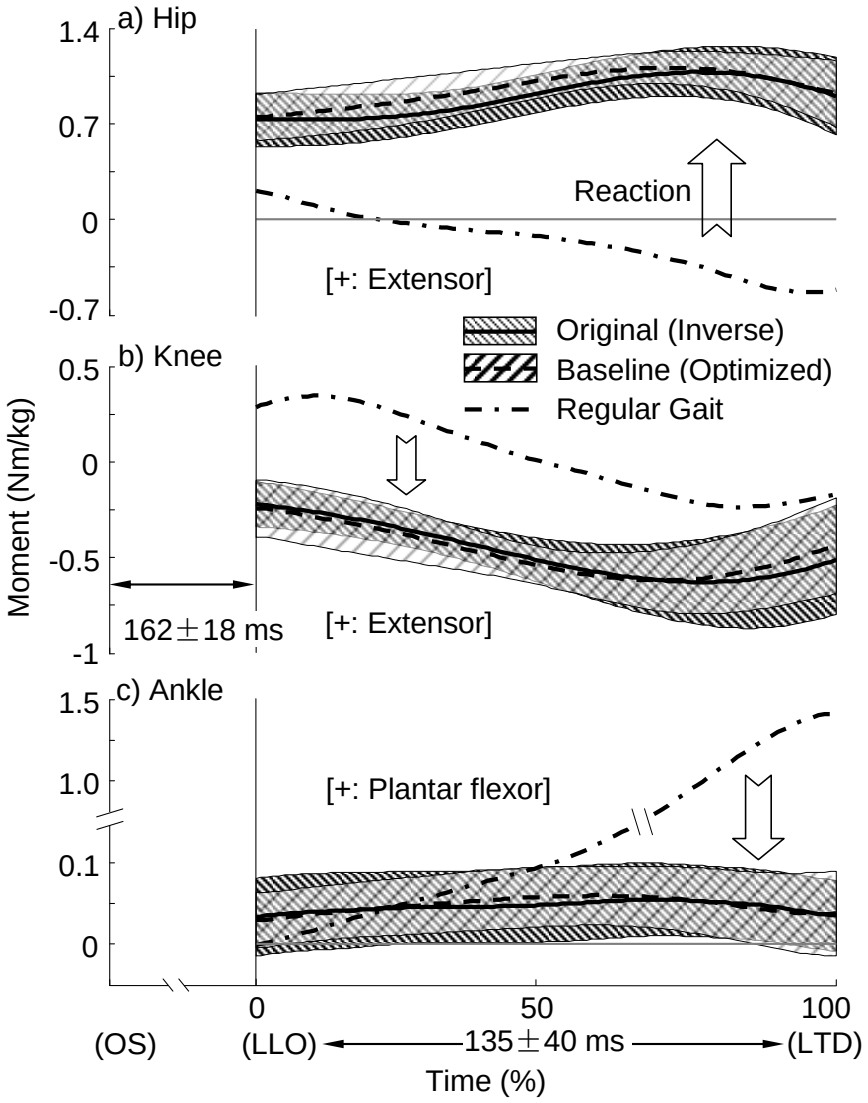

Fig. 3 [Yang and Pai, 2010]

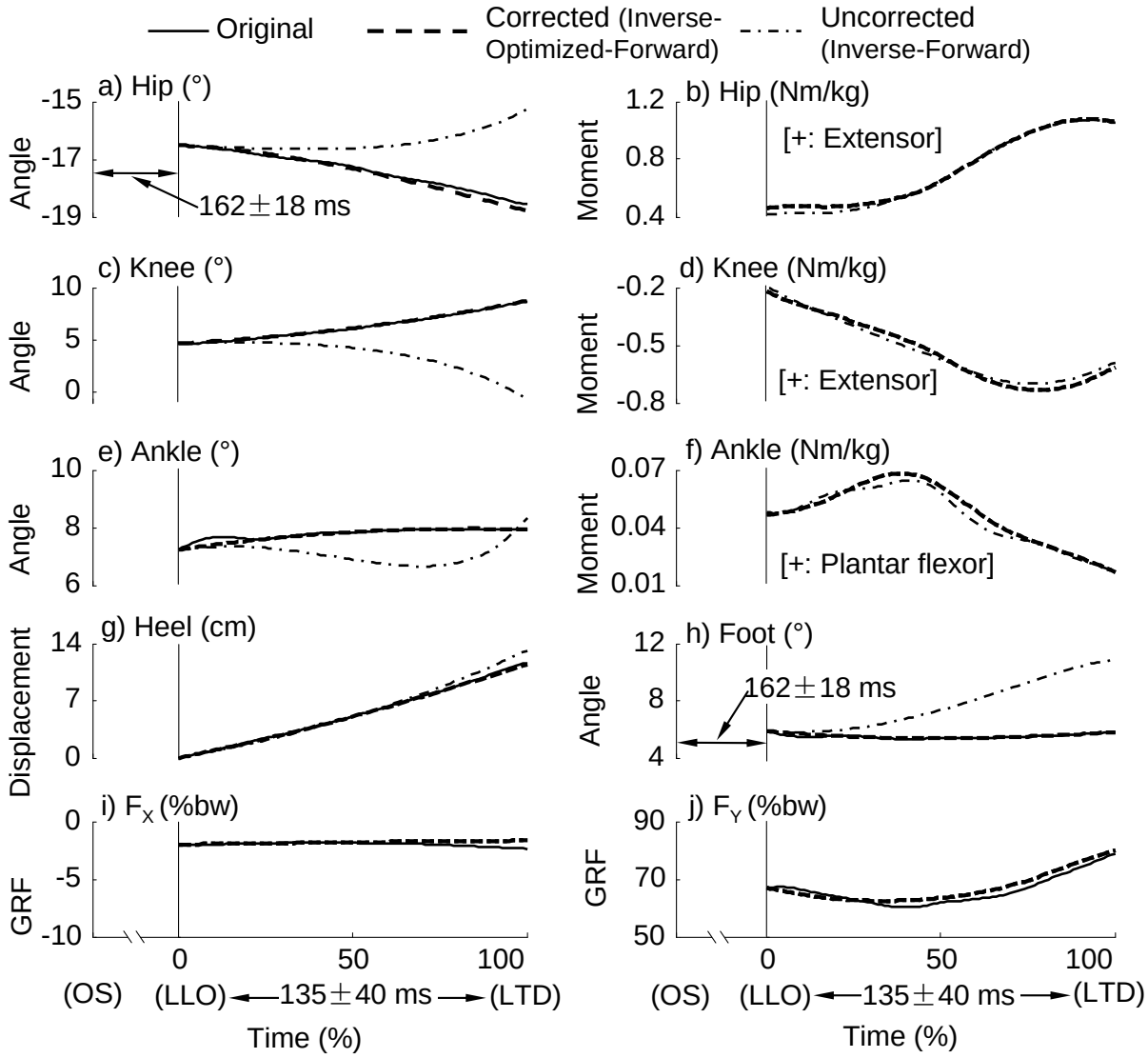

Fig. 4 [Yang and Pai, 2010]

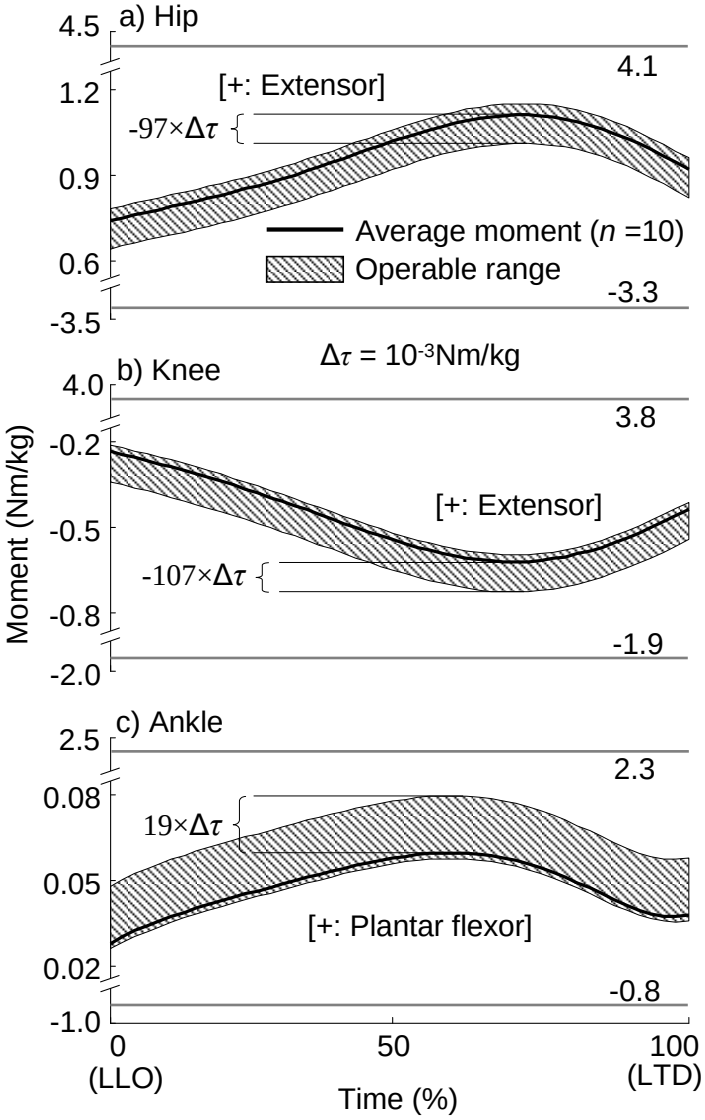

Fig. 5 [Yang and Pai, 2010]

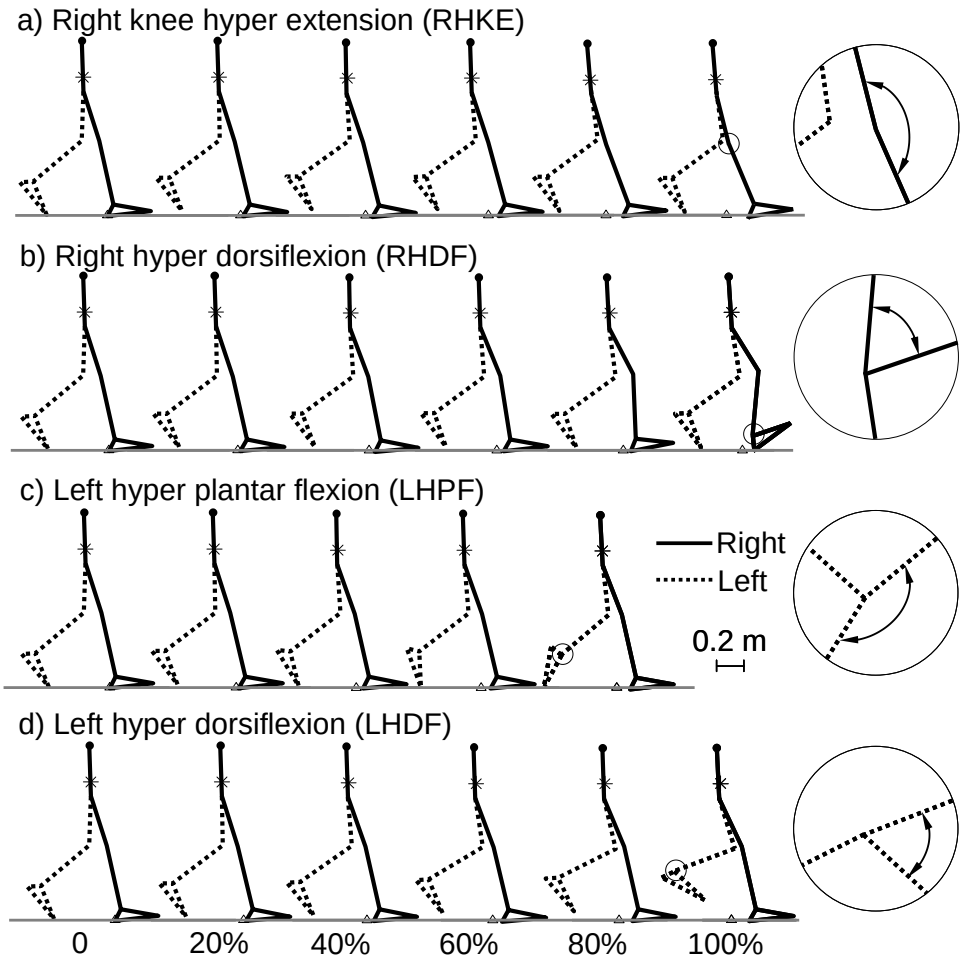

Fig. 6 [Yang and Pai, 2010]

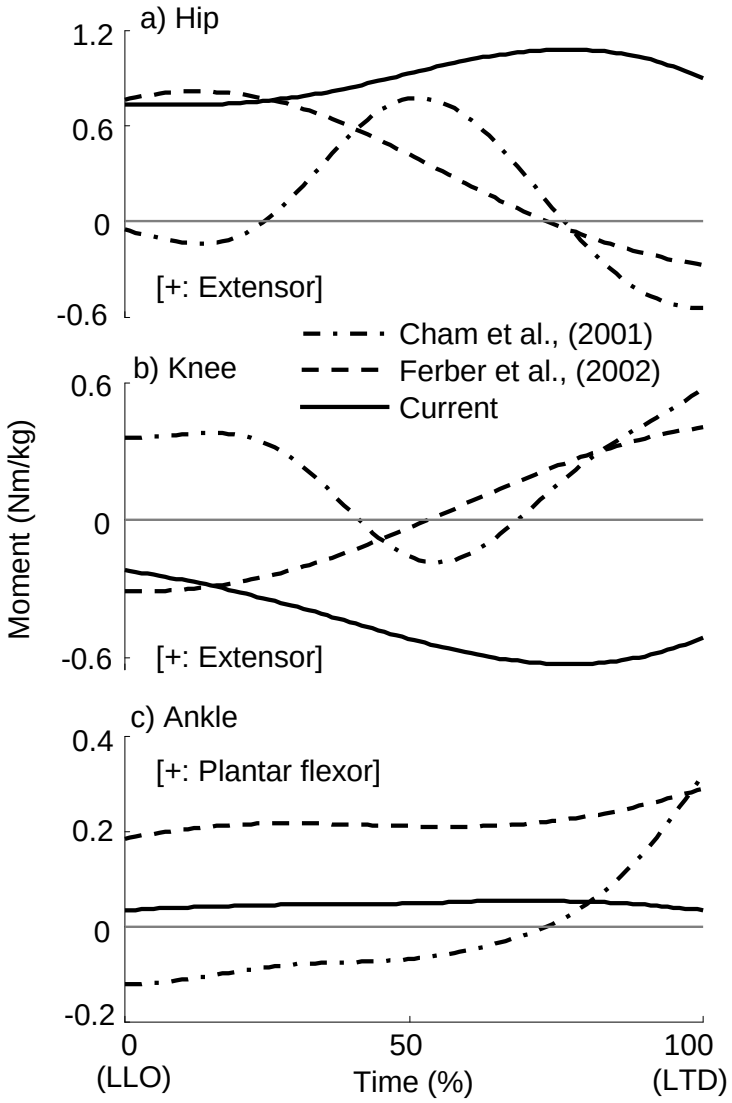

Fig. 7 [Yang and Pai, 2010]

APPENDIX

A. The optimization procedure

Each joint activation level time history was divided into a set of independent, linearly interpolated variables or control nodes. The *initiation* of the control nodes for SA was the original joint moments derived from the inverse-dynamics analysis. Once the control nodes were determined, each joint moment history was reconstructed using linear interpolation (Eq. (2)). After the initiation, the forward-dynamics simulation was performed by integrating the equations of motion (Eq. (1)). The objective function (Eq. (3)) was then evaluated by comparing the

output kinematics with the corresponding experimental values. Based on the evaluation, the values of control nodes and spring/damping coefficient of the visco-elastic element would be adjusted by SA in light of its acceptance/rejection criteria. This iteration was continued until the improvement in the object function became less than 10^{-3} for 500 consecutive function evaluations. The optimization-derived joint moments were the *baseline* moments used to investigate the operation limits.